JOURNAL OF SOLID STATE CHEMISTRY 25, 101–105 (1978)

# The Thermoelectric Power in $In_2O_3$

J. H. W. DE WIT, J. VAN DER BOM, AND J. F. DE GROOT

*Inorganic Chemistry Department, University of Utrecht, Croesestraat 77A, Utrecht, The Netherlands*

Received September 26, 1977; in revised form, December 16, 1977

The *n*-type semiconductivity of $In_2O_3$ is confirmed by the sign of the Seebeck coefficient. From a comparison of Hall and Seebeck data a value of 0.14 $m_0$ is deduced for the density-of-states effective mass. The incorporation of divalent cations results in a higher absolute value of the Seebeck coefficient, which is reflected in the lower charge carrier concentration, in accordance qualitatively with the defect model for $In_2O_3$.

## Introduction

Single-crystalline and polycrystalline $In_2O_3$ are *n*-type semiconductors, as is indicated by the oxygen pressure dependence of the conductivity ($\sigma \sim P_{O_2}^{-1/6}$) (*1, 2*) and proved by the negative sign of the Hall coefficient (*3–6*). Measurements of the Seebeck coefficient were reported earlier by Arvin (*7*), but these measurements of polycrystalline pressed tablets were severely influenced by the lead content. Weiher (*4*) did publish Seebeck coefficient measurements, but did not give experimental details, which weakens the information. In order to check the sign of the charge carriers in an independent way, we performed measurements of the Seebeck coefficient on polycrystalline material, with the same density (60%) and purity as the samples we reported on earlier (*2, 3*).

Accepting a large polaron band conduction model for $In_2O_3$, which seems reasonable, bearing in mind the rather good mobility of the charge carriers (*3*), the charge carrier concentration can also be deduced from the Seebeck coefficient, provided the density-of-states effective mass is known and the material is nondegenerate. From a comparison of the Hall effect and Seebeck coefficient data after correcting the Seebeck data for the transport factor, a value for the effective mass can be found. These values are compared with various literature data gathered by different techniques. The Seebeck coefficient of $In_2O_3$ is found to increase strongly when the material is doped with 1 wt% MgO, in accordance with our previously published defect model for $In_2O_3$ (*8*), which is based on oxygen vacancies as the majority ionic defect and the substitutional incorporation of Mg on In sites.

## Experimental

The preparation of the polycrystalline materials has been described elsewhere (*2*). All materials were prepared from the same $In_2O_3$ powder (Kawecki, 99.999%). A spectrochemical analysis of the materials showed impurity contents smaller than 0.1 ppm with the exception of 0.3 ppm for Fe and Al. For the Seebeck coefficient measurements, the powders were pressed into cylindrical rods of 1.5-cm length using a pressure of 3 ton $cm^{-2}$. The rods were sintered on $Al_2O_3$ plates at 1300°C overnight, and thereafter they were

022–4596/78/0251–0101$02.00/0

slowly cooled to room temperature. The Seebeck coefficient was measured with the following equipment. The samples were mounted in a quartz cell, as shown schematically in Fig. 1. A gas stream could be passed through the cell. The platinum electrodes were pressed onto the sample at a constant pressure by means of a spring. To obtain good contacts the surface of the sample was smoothly polished. No electrode contact paint was used, as contacts proved to be ohmic without it. The temperature gradient over the sample was arranged by means of two furnaces. These furnaces were fed by two Eurotherm P.I.D. temperature-control units which were modified in order to be driven externally via two potentiometers, coupled with a small motor, with variable speed. The temperature gradient could be kept constant with this equipment over the entire experimental temperature range.

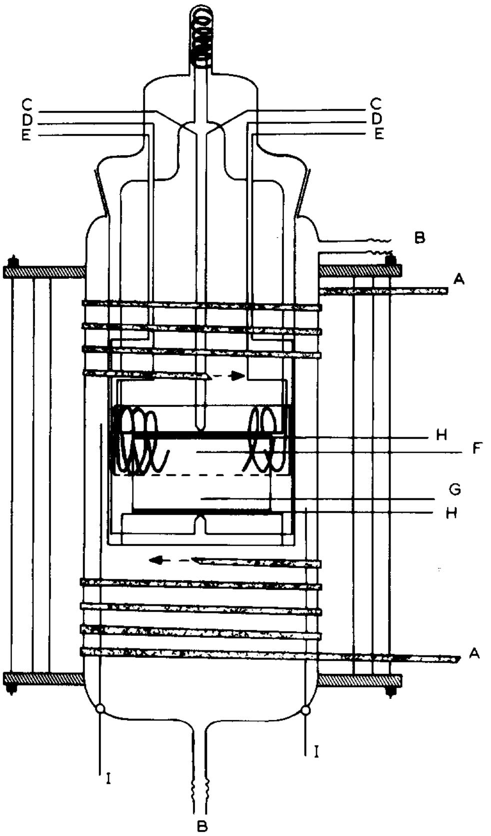

FIG. 1. The Seebeck cell; the quartz cell can be used for measurements from 25 to 800°C under various ambient conditions. The electrode pressure is regulated by means of a spring. A: Kantal wound furnace; B: gas in- and output; C: platinum–platinel (Engelhardt) thermocouple, Pt electrode lead; D: windings of small inner furnace; E: platinum–platinel thermocouple, Pt electrode lead; F: small inner furnace; G: sample; H: Pt electrodes.

A scheme of the detection unit is shown in Fig. 2. The upper and lower temperature signals and the Seebeck potential are fed to three channels of a datalogger (**5** in Fig. 2.) with an input impedance of 100 k$\Omega$ that is connected via a parallel-to-serial converter (**3**), a timer/scaler (**2**), and a printout control unit (**1**) to a teletype printer (**4**). The three signals were printed out every 20 min, while the temperature decreased linearly with time at a rate of 1°C/min. The measurements were always performed with cooling from 800°C after equilibration at this temperature for 1 hr.

The Hall effect equipment and the experimental procedures have been described in detail elsewhere (*3*).

## Results

Figure 3 shows the measured Seebeck coefficient on undoped and doped (1 wt% MgO) $In_2O_3$ as a function of the temperature

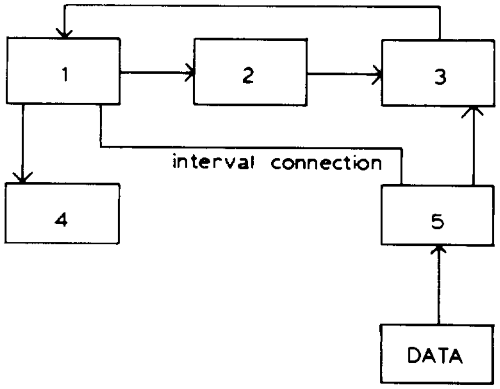

FIG. 2. The Seebeck effect detection unit. **1**: ORTEC PRINT OUT CONTROL (432); **2**: ORTEC TIMER/SCALER (431); **3**: ORTEC parallel/serial CONVERTER (702); **4**: TELETYP; **5**: ETROMETA DATALOGGER (E 13120).

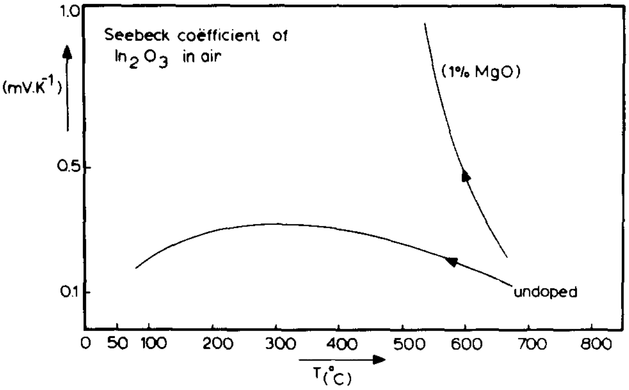

FIG. 3. The Seebeck coefficient of $In_2O_3$ as a function of the temperature in air.

in air. The sign of the Seebeck effect was negative for all samples, while the absolute value increased when the samples were doped with MgO. As a result of the steep increase of the signal for the sample doped with 1% MgO, which coincides with an enormous increase in resistance of the sample, the Seebeck effect was traced down to only 550°C. Below this temperature the measured values were unreliable (cf. Experimental).

## Discussion of Undoped Material

For an extrinsic nondegenerate *n*-type semiconductor the Seebeck coefficient can be given by

$$\varepsilon = -\frac{k}{e}\left(\frac{Q}{kT} + \ln\frac{N_C}{n_S}\right), \qquad (1)$$

where $Q$ denotes the heat of transfer, $k$ the Boltzmann constant, $e$ the free electron charge, $T$ the absolute temperature, $n_S$ the electron concentration, and $N_C$ the effective density-of-states function. The heat of transfer $Q$ is connected with the kinetic energy:

$$Q = AkT, \qquad (2)$$

where $A$ is a constant, depending on the dominant scattering mechanism. Accepting the broadband model for $In_2O_3$, the scattering of charge carriers within the sintered grains is probably determined, at least at higher temperatures, by optical lattice vibrations, which give a value of about 2 for $A$ (*9*).

The effective density of states in the case of a large polaron band semiconductor is given by

$$N_C = 2(2\pi m^* kT/h^2)^{3/2}, \qquad (3)$$

where $m^*$ denotes the polaron effective mass, and $h$ the Planck constant. From Eqs. (1) and (2) with $A = 2$,

$$n_S = N_C \exp 2 \exp(\varepsilon e/k). \qquad (4)$$

With Eq. (4) and accepting as a first approximation $m^* = m_0 \equiv$ the free electron mass, the data for undoped $In_2O_3$ as given in Fig. 3 were transformed to curve 1 in Fig. 4, which shows the electron concentration as a function of the reciprocal temperature. Curve 2 in Fig. 4 shows the electron concentration as obtained from the Seebeck coefficient without the correction for the contribution from the transport factor. The importance of this factor is obvious. In the same figure the electron concentration for undoped identical material as obtained from the Hall coefficient is given (curve 3). Because the expression for the Hall concentration does not contain any assumption on the effective mass, a combination of $n_{\mathrm{Hall}}$ with Eq. (4) gives for $m^*$ the expression

$$\frac{m^*}{m_0} = \left(\frac{n_{\mathrm{Hall}}}{n_S}\right)^{2/3}. \qquad (5)$$

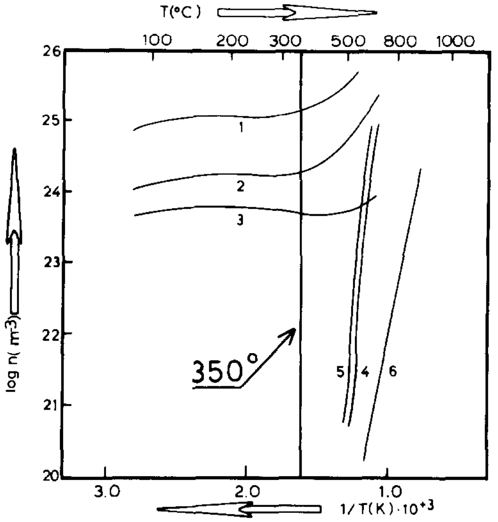

FIG. 4. The electron concentration as a function of the reciprocal temperature. curve 1: undoped material, $m^* = m_0$, $A = 2$; curve 2: undoped material, $m^* = m_0$, $A = 0$; curve 3: undoped material, from the Hall effect; curve 4: doped with 1% MgO, $A = 0$, $m^* = m_0$; curve 5: doped with 1% MgO, $A = 2$, $m^* = m_0$; curve 6: theoretical curve for 1% MgO-doped sample according to Eq. (7).

With Eq. (5) from curves 1 and 3 in Fig. 4 a value of 0.14 for $m^*/m_0$ is deduced. This is only done for the temperature range up to 350°C, where the two curves are parallel. Because the dynamic Hall coefficient measurements and the static Seebeck coefficient measurements respond in different manners to all surface effects (grain boundaries, depletion layers, etc.) this parallellism proves that these effects may be neglected for these samples, pretreated at 700°C in air! Above 350°C the starting evolution of oxygen may result in small changes in lattice dimensions, which is reflected in the different behaviors of the curves. This value is in reasonable agreement with literature data obtained by various techniques, as can be seen in Table I (*4, 5, 10*).

## Discussion of the Doped Material

After applying Eq. (4) to the Seebeck coefficient data for the doped material as given in Fig. 3, curves 4 and 5 in Fig. 4 result resp. when the transport factor $A$ is neglected and when it is not. In correcting these values by introducing 0.14 for the ratio $m^*/m_0$ in Eq. (4), an overall decrease of the electron concentration by a factor of 0.05 results (not given in Fig. 4). The observed decrease of the electron concentration by doping with MgO can be explained by the incorporation mechanism (*8*)

$$2\mathrm{MgO} \rightarrow 2\mathrm{Mg}'_{\mathrm{In}} + 2\mathrm{O}^{x}_{\mathrm{O}} + V^{\cdot\cdot}_{\mathrm{O}}. \qquad (6)$$

The defect model for $In_2O_3$ as published previously (*8*) gives the following expression for the quantitative influence of the dope concentration on $n$:

$$n = 1.41 \times K_{ox}^{1/6} \times P_{\mathrm{O}_2}^{-1/4} \times [\mathrm{Mg}'_{\mathrm{In}}]^{-1/2}, \qquad (7)$$

where $K_{ox}$ denotes the equilibrium constant for the nonstoichiometric decomposition of $In_2O_3$ (*8, 11*). Curve 6 in Fig. 4 represents the data obtained from Eq. (7) for an intended dope of 1% MgO, which was shown to represent in reality a concentration of $4 \times 10^{20}$ cm$^{-3}$ (*8*).

This curve does not fit the experimental data given in Fig. 4 even after correction by a factor of 0.05. This leads to the conclusion that the experimental points for the doped samples do not represent true equilibrium. This opinion is

TABLE I

A SURVEY OF LITERATURE DATA ON THE DENSITY-OF-STATES EFFECTIVE MASS IN $In_2O_3$

| $m^*/m_0$ | Method | Author | Year | Ref. |
|---|---|---|---|---|
| 0.55 | Hall + Seebeck (single crystal) | Weiher | 1962 | (*4*) |
| 0.50 ± 0.05 | Fundamental absorption edge (film) | Vainshtein Fistul' | 1967 | (*10*) |
| 0.30 | Electrical susceptibility + Hall (film) | Müller | 1968 | (*5*) |
| 0.14 | Hall + Seebeck (polycrystalline) | This work | 1978 | |

sustained by the fact that Hall effect measurements for this kind of material could not be performed reproducibly. The nonequilibrium situation may result from an incomplete incorporation of the MgO at these relatively low temperatures. In fact the added amount of MgO may well have exceeded the solubility limit of MgO at these temperatures in $In_2O_3$ because for different dope materials at these concentrations a second phase was observed with the scanning electron microscope (*12*).

## Conclusions

The *n*-type character of the charge carriers in $In_2O_3$ is confirmed by the Seebeck coefficient sign from room temperature to 700°C. From a comparison of Seebeck and Hall data, a value of 0.14 for the effective mass ratio $m^*/m_0$ is found, in reasonable agreement with literature data obtained by various techniques. The decreasing electron concentration during the incorporation of divalent Mg ions is reflected in an increasing Seebeck coefficient. The carrier concentration obtained from this coefficient cannot be correlated quantitatively with the incorporation model, probably because not all the MgO is incorporated and therefore a true equilibrium situation is not reached.

## Acknowledgment

Thanks are due to Mr. L. Louwerse, Mr. F. Pater, and Mr. H. Trommar for designing essential parts of the equipment.

## References

1. G. Rupprecht, *Z. Phys.* **139**, 504 (1954).
2. J. H. W. de Wit, *J. Solid State Chem.* **8**, 142 (1973).
3. J. H. W. de Wit, G. van Unen, and M. Lahey, *J. Phys. Chem. Solids* **38**, 819 (1977).
4. R. L. Weiher, *J. Appl. Phys.* **33**, 9, 2834 (1962).
5. H. K. Müller, *Phys. Status. Solidi* **27**, 723 (1968).
6. V. F. Korzo and V. N. Chernyayev, *Phys. Status Solidi A* **20**, 695 (1973).
7. M. J. Arvin, *J. Phys. Chem. Solids* **23**, 1681 (1962).
8. J. H. W. de Wit, *J. Solid State Chem.* **20**, 143 (1977).
9. A. J. Bosman and H. J. v. Daal, *Advan. Phys.* **19**, No. 77, 1 (1970).
10. V. M. Vainshtein and V. I. Fistul', *Sov. Phys. Semicond.* **4**, 8, 1278 (1971).
11. J. H. W. de Wit, *J. Solid State Chem.* **13**, 192 (1975).
12. J. H. W. de Wit, M. Lahey, and P. F. Elbers, presented at the 9th European Conference on the Science of Ceramics, Noordwijkerhout, The Netherlands, 13–16 November 1977.